NATIONAL ADVISORY COMMITTEE FOR AERONAUTICS

TECHNICAL NOTE 3374

TURBULENT-HEAT-TRANSFER MEASUREMENTS AT A MACH NUMBER OF 2.06

By Maurice J. Brevoort and Bernard Rashis

Langley Aeronautical Laboratory
Langley Field, Va.

Washington

March 1955

1D

NATIONAL ADVISORY COMMITTEE FOR AERONAUTICS

TECHNICAL NOTE 3374

TURBULENT-HEAT-TRANSFER MEASUREMENTS AT A MACH NUMBER OF 2.06

By Maurice J. Brevoort and Bernard Rashis

SUMMARY

Turbulent-heat-transfer measurements were obtained through the use of an axially symmetric annular nozzle which consists of an inner shaped center body and an outer cylindrical sleeve. Measurements taken along the outer sleeve gave essentially flat-plate results that are free from wall interference and corner effects for a Mach number of 2.06 and for a Reynolds number range of 1.7×10^6 to 8.8×10^7. The heat-transfer coefficients are in good agreement with available data from V-2 rockets and also check the Rubesin theory and the Van Driest theory for a Mach number of 2.0 and for a ratio of inner-surface to free-stream temperature of 1.8. The temperature-recovery factors are approximately 0.5 percent lower than the factors given in NACA TN 2077 for a Mach number of 2.4.

INTRODUCTION

The design of supersonic aircraft and missiles requires engineering information about heat-transfer coefficients and temperature-recovery factors for supersonic speeds that extend over a wide range of Reynolds number. In reference 1, local-heat-transfer-coefficient measurements were presented for a Mach number of 3.03. Good agreement of these results with theoretical and experimental work was obtained. This method of testing and reduction of data is readily adaptable to obtaining accurate measurements over an extended range of both Mach and Reynolds numbers.

The purpose of this investigation is to extend the work initiated in reference 1 to a Mach number of 2.06. The same type of apparatus and method of reducing the data were used in this investigation as were employed in reference 1. The range of Reynolds number for which measurements were obtained is from 1.7×10^6 to 8.8×10^7. The results cover a temperature difference of approximately 20° at 40 seconds after starting to approximately 5° at 120 seconds after starting. The average value of the ratio of inner-surface temperature to free-stream temperature T_w/T_∞ was 1.8.

SYMBOLS

c	specific heat of sleeve material, Btu/lb-$^{\circ}$R
c_p	specific heat of air at constant pressure, Btu/lb-$^{\circ}$R
g	acceleration due to gravity, ft/sec^2
h	heat-transfer coefficient, Btu/ft^2-sec-$^{\circ}$R
k	heat conductivity, Btu/ft-sec-$^{\circ}$R
M	Mach number
Nu	Nusselt number, hx/k
Pr	Prandtl number, $\mu c_p g/k$
R	Reynolds number, $\rho V x/\mu$
St	Stanton number, $\frac{Nu}{R\ Pr} \equiv \frac{h}{\rho V c_p g}$
T_{av}	average wall temperature, $^{\circ}$R
T_e	effective stream air temperature at wall, some temperature which gives a thermal potential which is independent of heat-transfer coefficient h, $^{\circ}$R
T_t	stagnation temperature, $^{\circ}$R
T_w	inside-surface temperature of nozzle sleeve, $^{\circ}$R
T_∞	free-stream temperature, $^{\circ}$R
t	time, sec
V	free-stream velocity, ft/sec
w	specific weight of sleeve material, lb/sq ft
x	longitudinal distance along sleeve, ft (unless indicated otherwise)

η_r recovery factor, $\frac{T_e - T_\infty}{T_t - T_\infty}$

μ dynamic viscosity coefficient, lb-sec/sq ft

ρ free-stream density of air, slugs/cu ft

APPARATUS AND METHOD

The apparatus consisted of an axially symmetric annular nozzle which was directly connected to the settling chamber of one of the cold-air blowdown jets of the Langley gas dynamics laboratory. The nozzle had a shaped wooden center body and two outer sleeves. The first sleeve was constructed from 8-inch-diameter, extra heavy, seamless carbon-steel pipe and the second was constructed from 1/16-inch stainless steel which was rolled into a cylinder and welded; both were surfaced-machined inside and outside to a wall thickness of 0.388 inch and 0.060 inch, respectively. A detailed drawing of the apparatus is shown in figure 1 which gives the location of the thermocouples and the static-pressure orifices. Several static-pressure orifices and thermocouples were located 90° apart around the sleeve to calibrate the flow for axial symmetry. The coordinates of the center body are given in table I. The center body was designed by using three-dimensional characteristics. (See ref. 2.) Station locations, shown in figure 1, refer to the distance in inches from the nozzle minimum station.

Details of the installation of the thermocouples and static-pressure orifices are shown in figures 2 and 3. The thermocouples are located 0.060 inch from the inner surface of the sleeve. The wires are 30-gage copper-constantan (0.010 inch in diameter); conduction along the wire length is negligible. As indicated in figure 2, the thermocouples are in intimate contact with the steel wall so that thermal resistance at this junction is negligible.

The Mach number distribution was measured both lengthwise and around the sleeve. The orifices located around the sleeve were used to check the alinement of the center body within the sleeve. The results are shown in figure 4 and are accurate to ±0.01.

The temperature-recording equipment consisted of three synchronized high-speed self-balancing Brown ElectroniK strip chart recorders, having a total of 36 switches, two of which were connected to the settling-chamber thermocouples and the others were connected to the sleeve thermocouples.

A typical test consisted of operating the nozzle at the desired pressure. The stagnation temperature starts at essentially room temperature and decreases as the piping is cooled, as illustrated in figure 5 where stagnation temperature is plotted against time for a settling-chamber pressure of 106 lb/sq in. gage. The wall temperature also starts at essentially room temperature and tends to approach the equilibrium temperature which is approximately 25° F below stagnation temperature. This variation is shown in figure 6 where wall temperature is plotted against time for stations 12 and 18 for a settling-chamber pressure of 106 lb/sq in. gage. Test runs were made for settling-chamber pressures of 1, 38, 106, and 185 lb/sq in. gage. The test at a pressure of 1 lb/sq in. gage was made with a sleeve 0.060 inch thick, and the test setup was evacuated to an absolute pressure of 1.0 inch of mercury. Except for the first 20 seconds, the pressures were maintained constant for each test run. The recorders were calibrated immediately before and after each run and were found to be accurate to ±1° F.

In figure 7 are plotted, for various times during the test run, the values of wall temperature against longitudinal distance along the cylinder. These values were used to determine the rate of change of the longitudinal conduction $k \frac{d^2T_{av}}{dx^2}$ along the cylinder. Test results were taken only for the length of the cylinder for which $k \frac{d^2T_{av}}{dx^2}$ was zero.

REDUCTION OF DATA

Short test runs in which time histories of the wall temperature are obtained give the essential data from which heat-transfer coefficients and temperature-recovery factors may be determined. The reduction of these data requires a method in which the stagnation temperature, and accordingly the equilibrium temperature, may vary in an arbitrary manner.

The Stanton number is calculated from

$$St = \frac{h}{\rho V c_p g} \tag{1}$$

and the heat-transfer coefficient is calculated from

$$h = wc \frac{dT_{av}/dt}{T_w - T_e} \tag{2}$$

By definition, the recovery factor is

$$\eta_r = \frac{T_e - T_\infty}{T_t - T_\infty} \tag{3}$$

The method of reducing the data is simply to select a recovery factor and then obtain T_e from equation (3). Substitute this value of T_e into equation (2) and obtain values of h for different heat-flow rates. These values of h are then substituted into equation (1). The true values of T_e, η_r, and St are obtained when St is constant with time (for different heat-flow rates). Figure 8 shows the values used in evaluating the Stanton number and recovery factor at station 12 for a settling-chamber pressure of 106 lb/sq in. gage.

The values of specific heat and specific weight of the sleeve material were taken from reference 3. The values of viscosity and Prandtl number (0.71) for air were also taken from reference 3 and were based upon the inside-surface temperature of the sleeve. The value of T_w chosen was at 80 seconds after starting. (This arbitrary choice of temperature can be made since the viscosity coefficient is practically a constant factor of the heat-conduction coefficient.)

PRECISION OF EQUIPMENT

The basic data consist of time histories of temperature at each thermocouple location. The recorders were calibrated immediately before and after each run and were found to be accurate to $\pm 1^\circ$ F. The thermocouple wires are 30-gage (0.010-inch-diameter) copper-constantan and of such small diameter that conduction along their length can be neglected. The wires are insulated except at the junction where intimate contact with the sleeve keeps any thermal resistance to a minimum.

The sleeve is enclosed in a vacuum jacket to avoid free convection and, for the temperature range considered, radiation effects range up to 2 percent. The product of the specific weight and the specific heat of the sleeve material as used in equation (2) is accurate to ± 5 percent.

The value of $\frac{dT_{av}}{dt}$ used in equation (2) is that of the actual thermocouple reading, whereas it should be the value associated with the average temperature in the thickness of the sleeve at each point. During the test runs the inner-surface temperatures are lower than the average temperatures by approximately 1° to 1.5° at the beginning of the runs

(40 seconds after starting) and become the same at the end of the runs (150 seconds). This deviation causes the derivative of inner-surface temperature with time to be less than the derivative of average temperature with time by approximately 1 percent.

The analysis of reference 4 was used to determine the effect of the sleeve diameter upon the flow characteristics. This effect was computed to be less than one-hundredth of 1 percent.

RESULTS AND DISCUSSION

Figure 7 shows the variation of wall temperature with longitudinal distance along the cylinder for a settling-chamber pressure of 106 lb/sq in. gage. Over the test range, the wall temperatures are constant along x. In the relation

$$h = \frac{wc\ dT_{av}/dt}{T_w - T_e}$$

w and c are constant and dT_{av}/dt is constant because T_w is constant. Therefore, if there is to be a variation of h with Reynolds number or x, T_e must vary with x. The value of T_e obtained for the test at a settling-chamber pressure of 106 lb/sq in. gage, evaluated at 80 seconds after starting, actually decreases approximately 1.5°.

Figure 9 shows the variation of local Nusselt number with local Reynolds number. The value of x used in evaluating these numbers was based upon an x that was considered to be zero at the nozzle minimum station. A single line faired through all the data points has a slope of approximately 0.8; but if lines are faired through the points for each settling-chamber pressure, the slopes are slightly higher. It is reasonable to assume, however, that the higher stagnation pressures would produce earlier transition and the zero value of x would move upstream with increasing stagnation pressure. Hence, if it is assumed that data from each settling-chamber pressure should merge into a continuous line (rather than a series of steps), x may be adjusted for zero x-locations (the effective beginning of the turbulent boundary layer) which would make all the test runs coincident. This adjustment has been made in figure 10 by using values of x equal to zero at 1.60 inches downstream of the nozzle minimum station for a settling-chamber pressure of 1 lb/sq in. gage and 2.00, 4.40, and 6.00 inches upstream of the minimum for the chamber pressures of 38, 106, and 185 lb/sq in. gage, respectively.

The Nusselt numbers were found to vary from 1,690 to 44,950 for the Reynolds number range of 1.7×10^6 to 8.8×10^7 (based on adjusted zero x-locations). For comparison, the curves based upon the analyses of Van Driest (ref. 5) and Rubesin (ref. 6) are shown. In the Van Driest analysis T_w/T_∞ was considered to be 1.8 (the average value of the test results). For comparison with these references, the data were computed by using free-stream temperature to determine the density and the velocity. The wall temperature was used to determine the viscosity and the Prandtl number. The experimental values from the data of V-2 rockets (ref. 7) are also determined in this manner. The Mach number range for the V-2 data in figure 10 is from 1.95 to 2.07. The agreement between the results of this investigation and those of references 5, 6, and 7 is good.

Figure 11 shows the variation of local temperature-recovery factor with local Reynolds number. The variation is from 0.891 at $R = 1.7 \times 10^6$ to 0.870 at $R = 8.8 \times 10^7$. The results are compared with a curve which represents the fairing of the data of reference 8. The data of reference 8 are for a Mach number of 2.4. The results obtained in this investigation are approximately 0.5 percent lower. Also included for comparison are the curves for recovery factor equal to $Pr^{1/3}$ and $Pr^{1/2}$. The wall temperature was used to determine the Prandtl number.

CONCLUDING REMARKS

Turbulent-heat-transfer measurements that gave essentially flat-plate results were obtained for a Mach number of 2.06 and for a Reynolds number range of 1.7×10^6 to 8.8×10^7. The Nusselt numbers are in good agreement with theoretical analyses and with experimental data obtained with the V-2 rockets. The temperature-recovery factors are approximately 0.5 percent lower than other available data for a Mach number of 2.4.

Langley Aeronautical Laboratory,
National Advisory Committee for Aeronautics,
Langley Field, Va., December 3, 1954.

REFERENCES

1. Brevoort, Maurice J., and Rashis, Bernard: Turbulent-Heat-Transfer Measurements at a Mach Number of 3.03. NACA TN 3303, 1954.

2. Ferri, Antonio: Elements of Aerodynamics of Supersonic Flows. The Macmillan Co., 1949.

3. Eckert, E. R. G. (With Appendix by Robert M. Drake, Jr.): Introduction to the Transfer of Heat and Mass. First ed., McGraw-Hill Book Co., Inc., 1950, pp. 266 and 274.

4. Beckwith, Ivan E.: Heat Transfer and Skin Friction by an Integral Method in the Compressible Laminar Boundary Layer With a Streamwise Pressure Gradient. NACA TN 3005, 1953.

5. Van Driest, E. R.: The Turbulent Boundary Layer for Compressible Fluids on a Flat Plate With Heat Transfer. Rep. No. AL-997, North American Aviation, Inc., Jan. 27, 1950.

6. Rubesin, Morris W.: A Modified Reynolds Analogy for the Compressible Turbulent Boundary Layer on a Flat Plate. NACA TN 2917, 1953.

7. Fischer, W. W.: Supersonic Convective Heat Transfer Correlations From Skin-Temperature Measurements During Flights of V-2 Rockets No. 19 and No. 27. Rep. No. 55258, Gen. Elec. Co., July 1949.

8. Stalder, Jackson R., Rubesin, Morris W., and Tendeland, Thorval: A Determination of the Laminar-, Transitional-, and Turbulent-Boundary-Layer Temperature-Recovery Factors on a Flat Plate in Supersonic Flow. NACA TN 2077, 1950.

TABLE I.- CENTER-BODY COORDINATES

x, in.	Radius, in.	x, in.	Radius, in.
-10.25	2.000	1.8	3.1787
-4.7	2.000	1.9	3.1618
-4.5	2.020	2.0	3.1456
-4.0	2.100	2.1	3.1303
-3.0	2.500	2.2	3.1157
-2.5	2.735	2.3	3.1020
-2.0	2.970	2.4	3.0890
-1.5	3.150	2.5	3.0769
-1.0	3.300	2.6	3.0655
-.8	3.340	2.7	3.0550
-.6	3.375	2.8	3.0453
-.4	3.400	2.9	3.0364
-.2	3.425	3.0	3.0283
0	3.4375	3.1	3.0211
.1	3.4364	3.2	3.0147
.2	3.4333	3.3	3.0091
.3	3.4280	3.4	3.0043
.4	3.4204	3.5	3.0004
.5	3.4108	3.6	2.9974
.6	3.3990	3.7	2.9952
.7	3.3852	3.8	2.9939
.8	3.3696	3.9	2.9934
.9	3.3522	4.0	2.9924
1.0	3.3336	5.0	2.9824
1.1	3.3141	10.0	2.9324
1.2	3.2941	15.0	2.8824
1.3	3.2739	20.0	2.8324
1.4	3.2538	25.0	2.7824
1.5	3.2341	30.0	2.7324
1.6	3.2149	34.0	2.6924
1.7	3.1964	34.250	2.6999

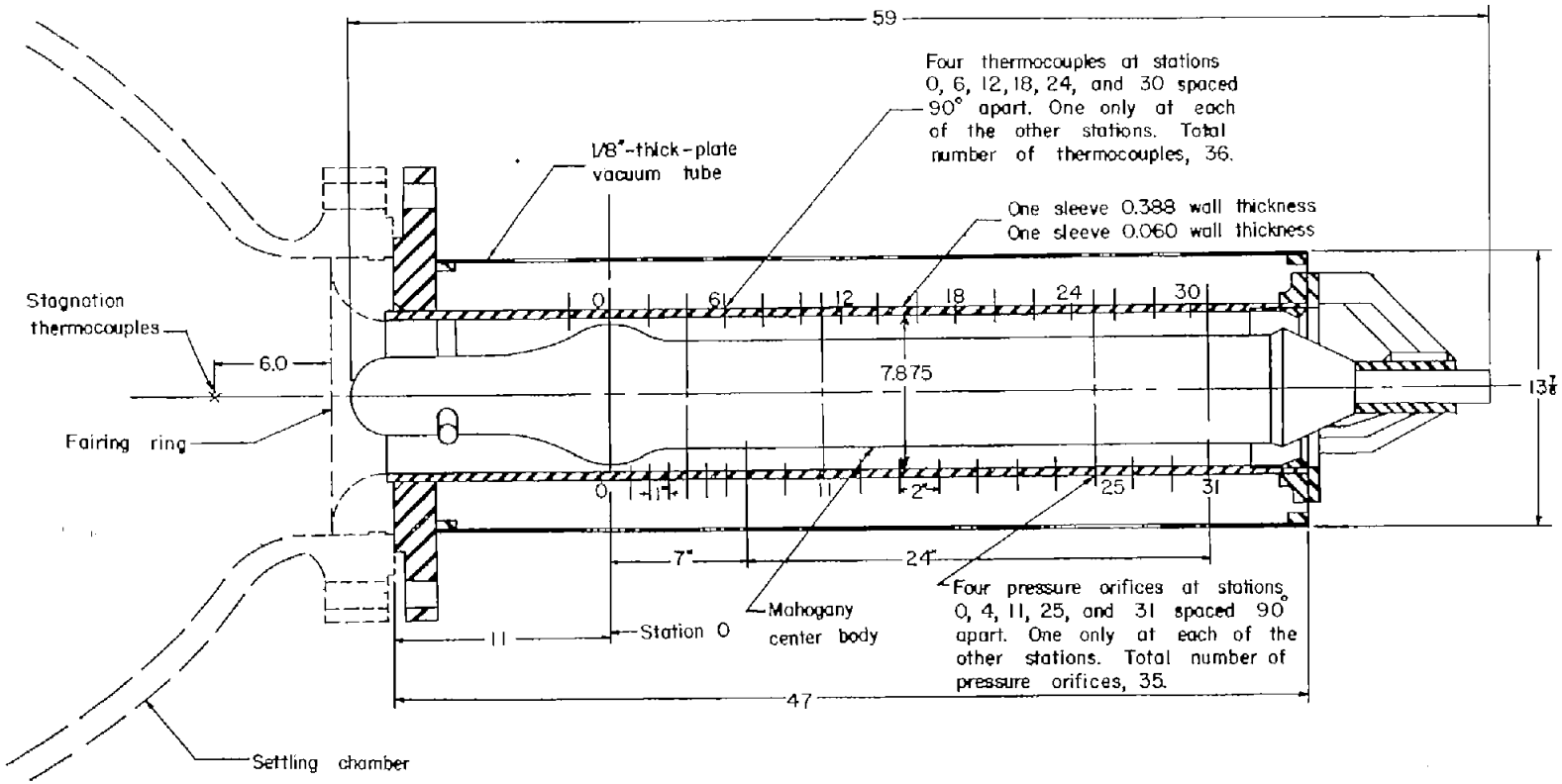

Figure 1.- Test arrangement. Dimensions are in inches.

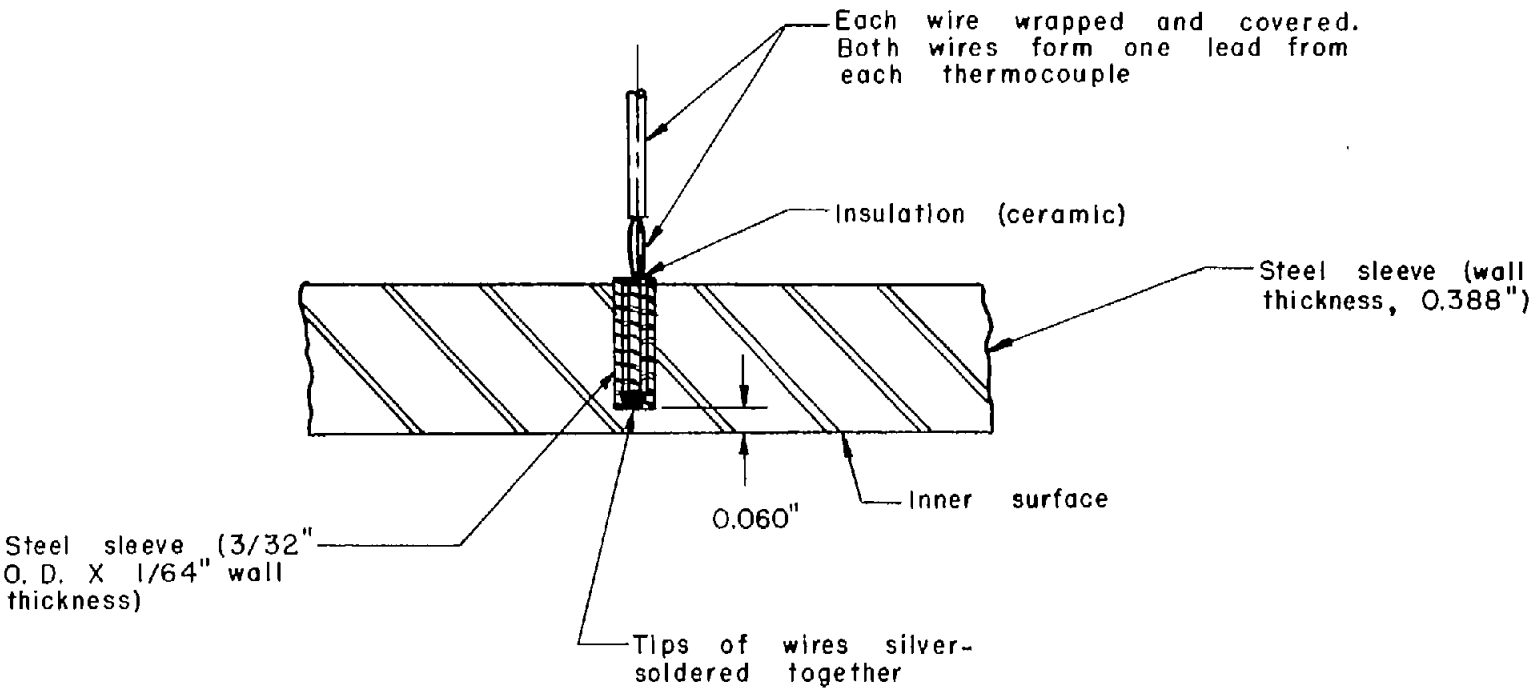

Figure 2.- Thermocouple installation.

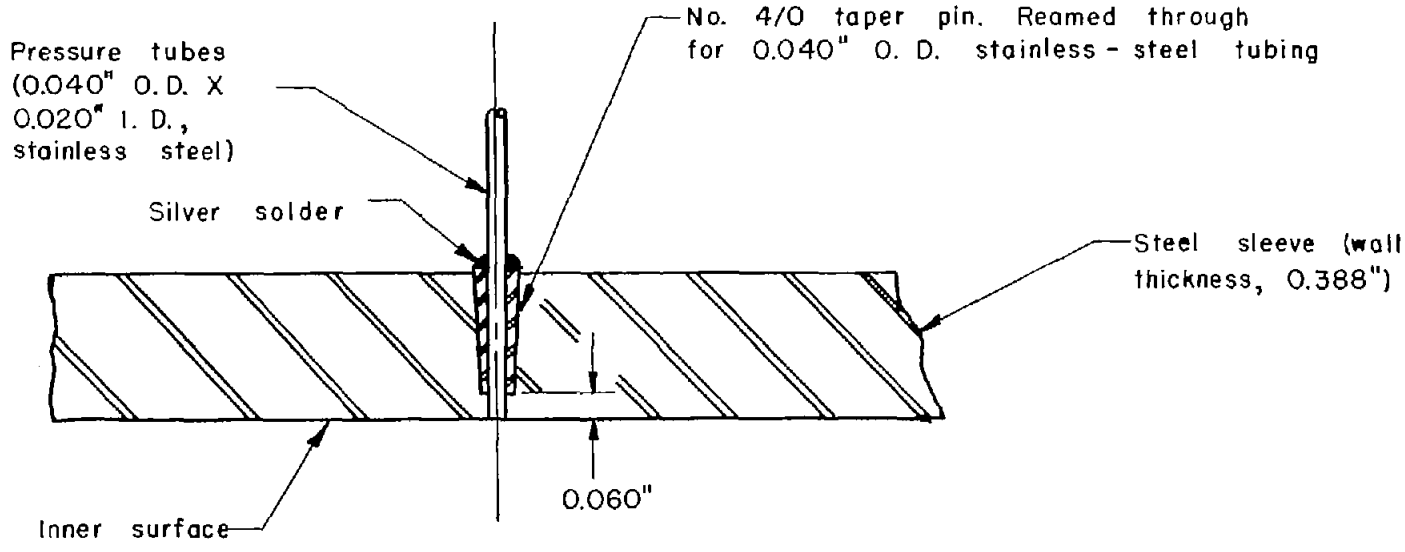

Figure 3.- Pressure-orifice installation.

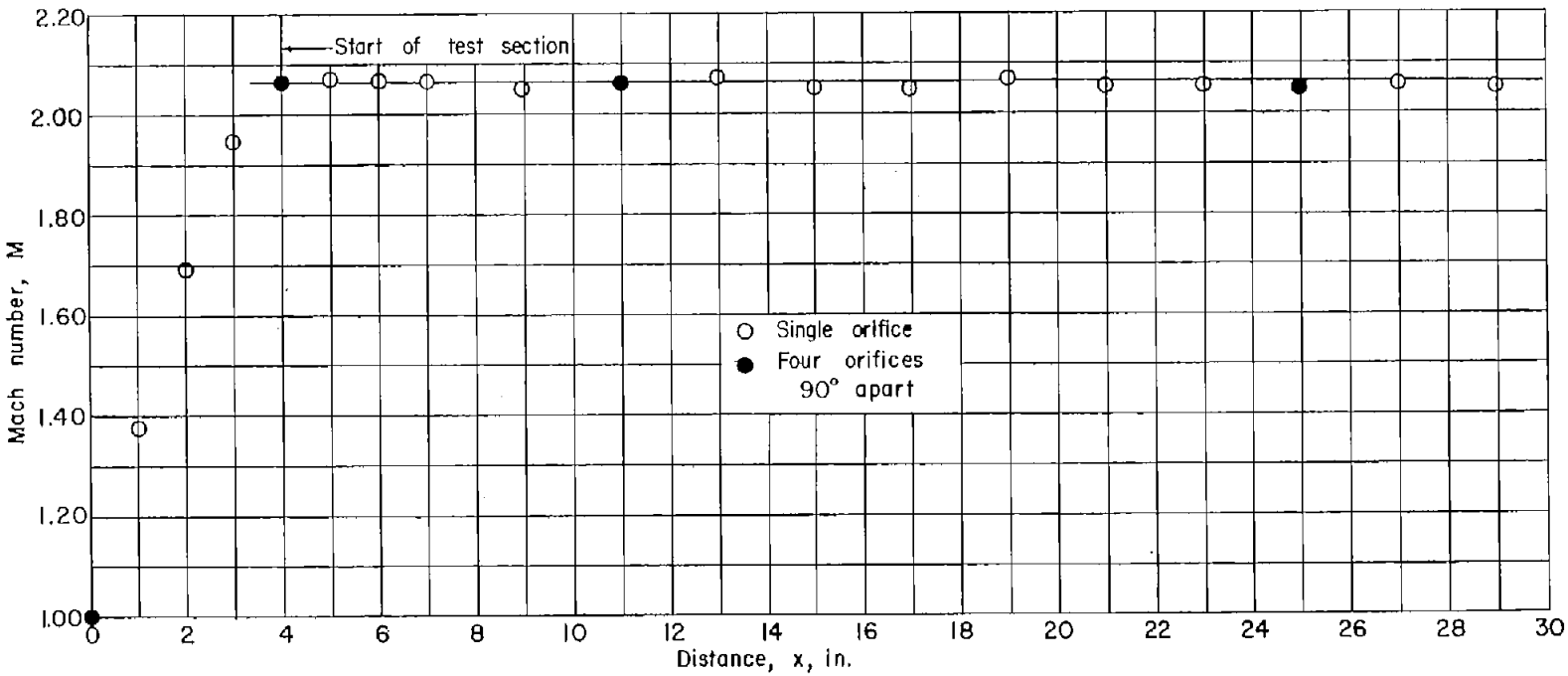

Figure 4.- Mach number distribution for settling-chamber pressure of 106 lb/sq in. gage.

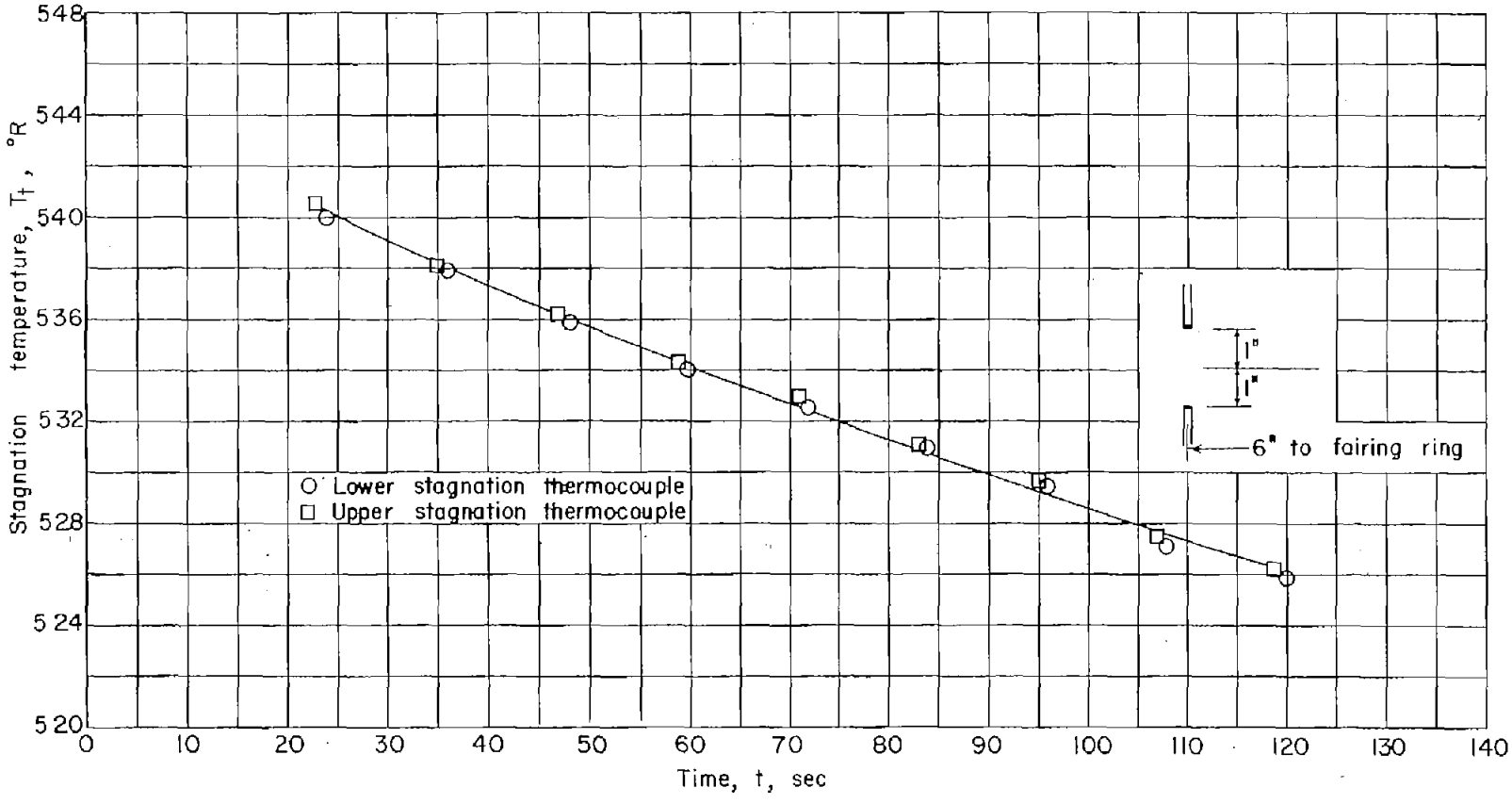

Figure 5.- Variation of stagnation temperature with time for a settling-chamber pressure of 106 lb/sq in. gage.

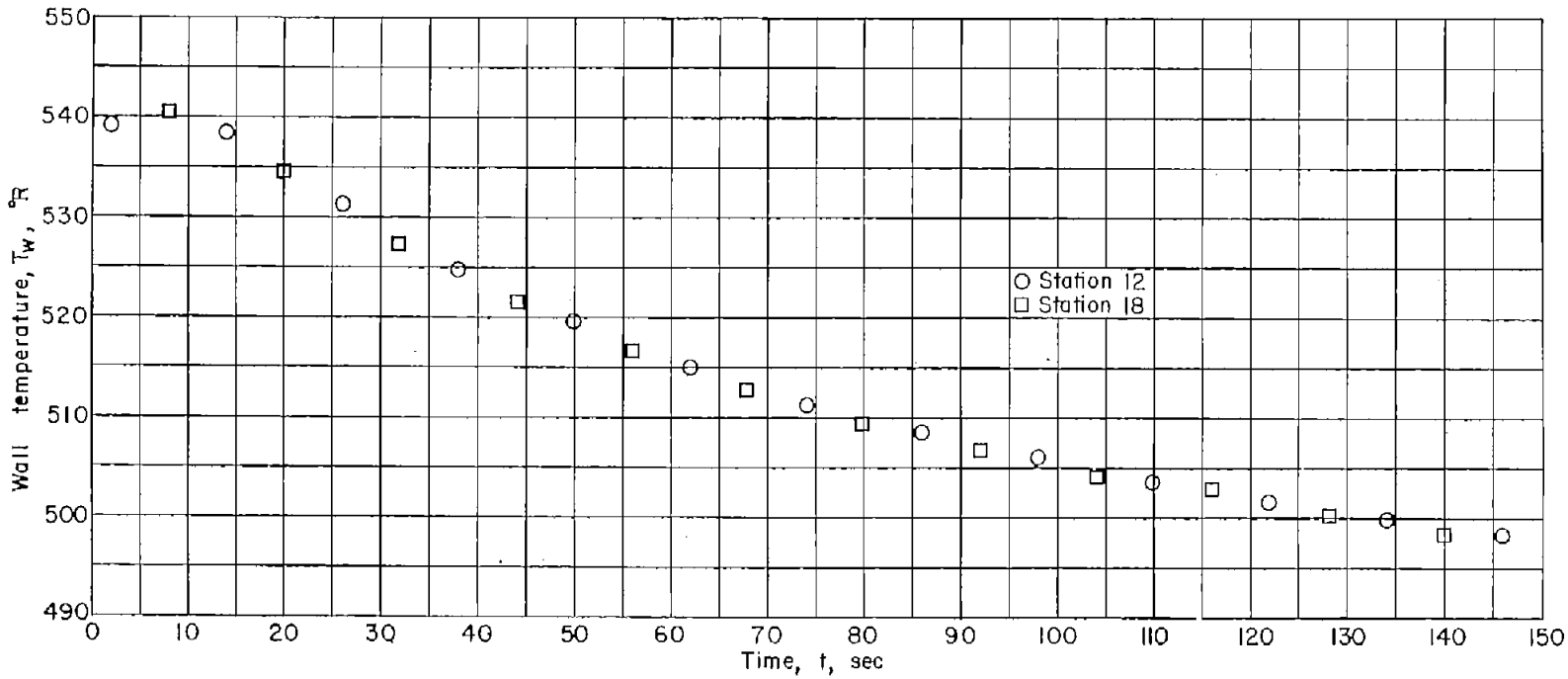

Figure 6.- Variation of wall temperature with time for a settling-chamber pressure of 106 lb/sq in. gage.

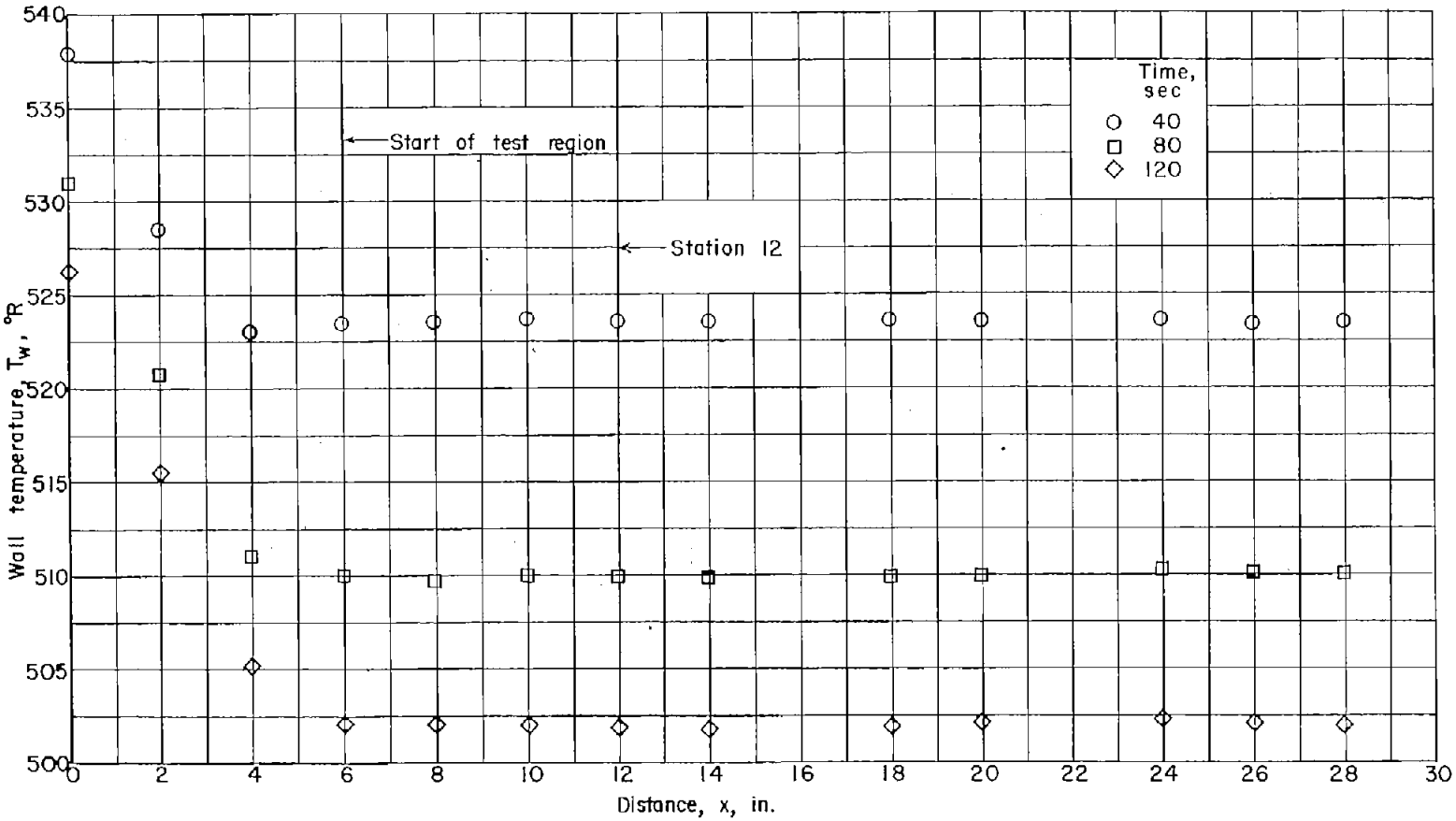

Figure 7.- Variation of wall temperature with longitudinal distance for a settling-chamber pressure of 106 lb/sq in. gage.

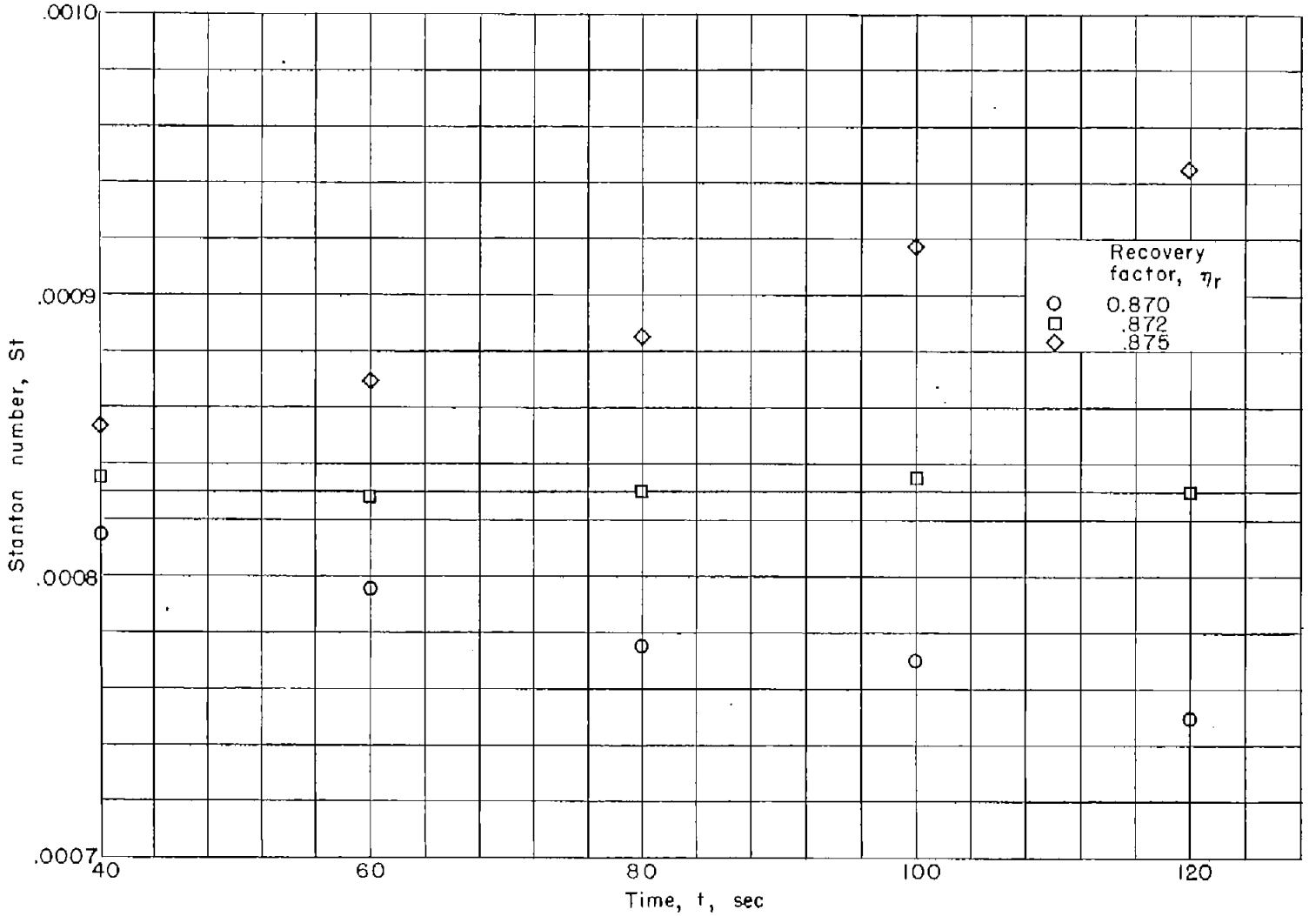

Figure 8.- Stanton number as a function of time and recovery factor for station 12 for a settling-chamber pressure of 106 lb/sq in. gage.

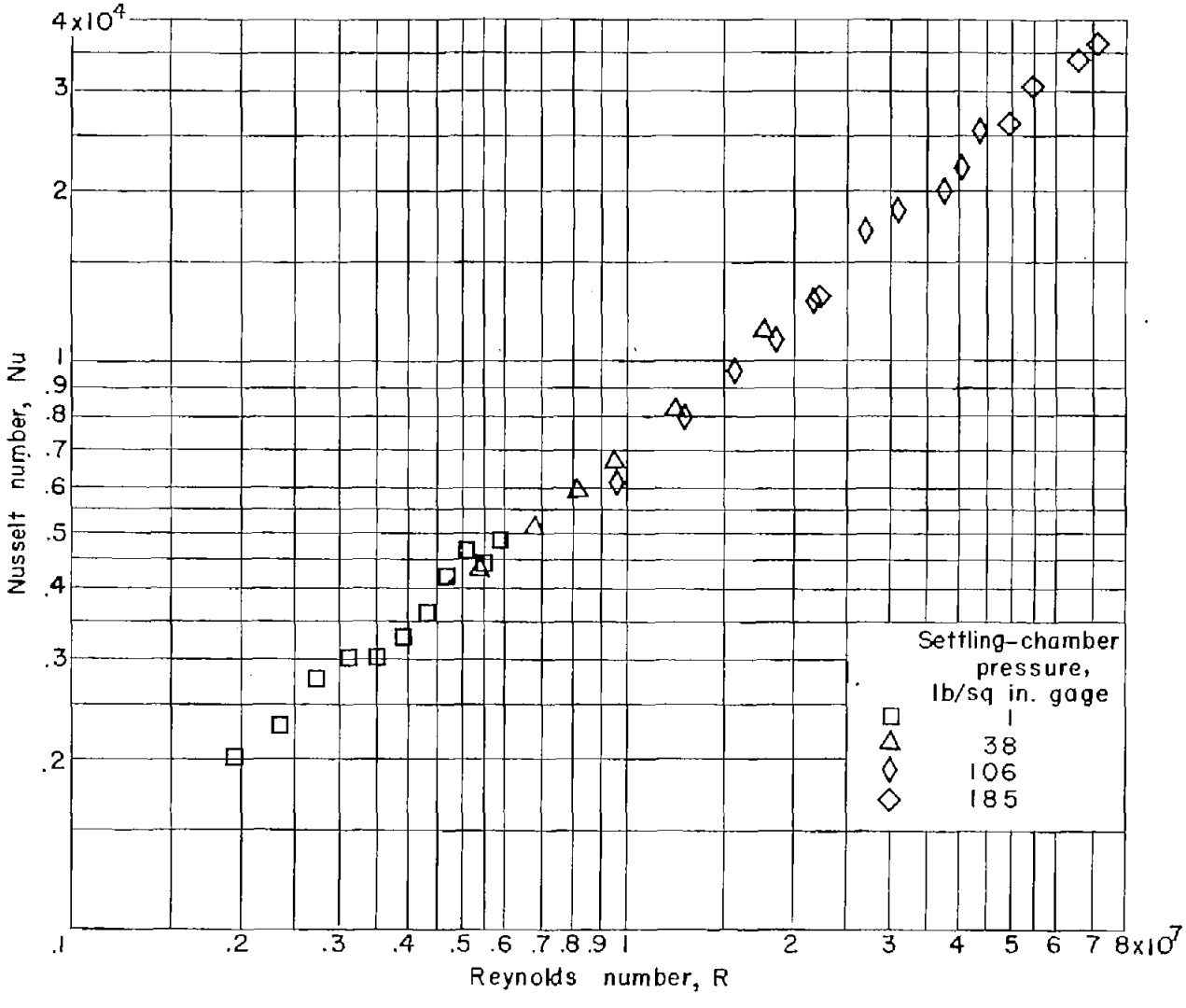

Figure 9.- Variation of local Nusselt number with local Reynolds number for $x = 0$ at station 0.

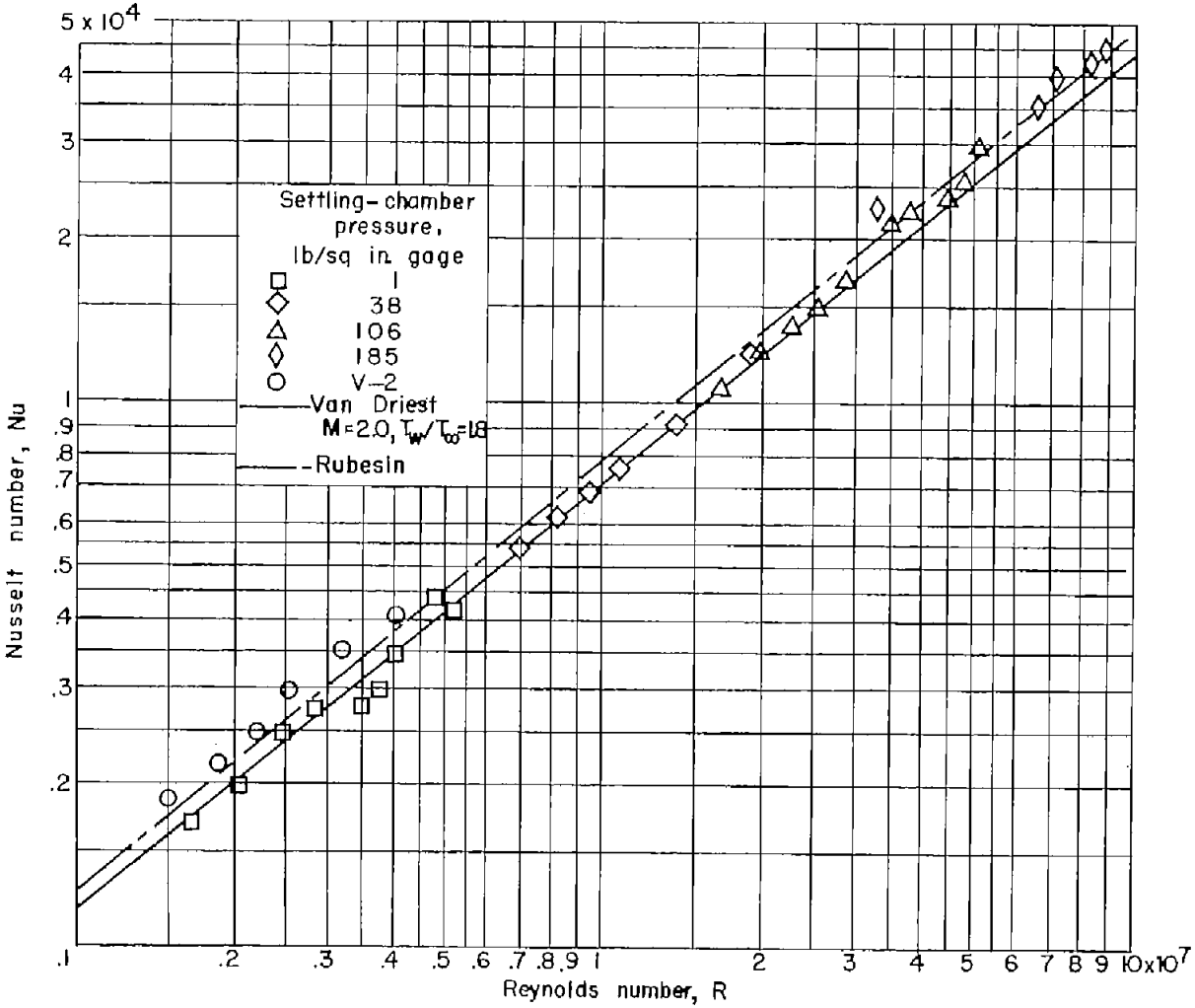

Figure 10.- Variation of local Nusselt number with local Reynolds number for corrected locations of x = 0. Viscosity and Prandtl number determined for wall temperatures.

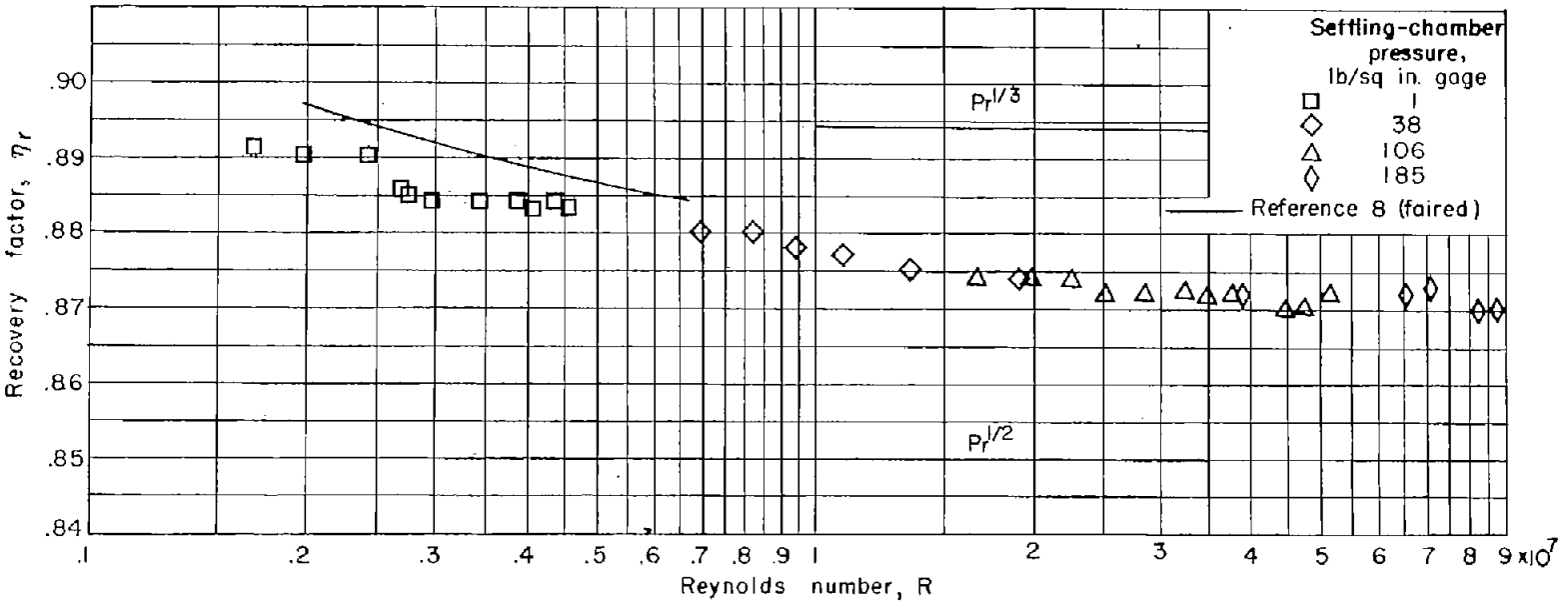

Figure 11.- Variation of local recovery factor with local Reynolds number for corrected locations of x = 0. Viscosity determined for wall temperatures.

NACA-Langley - 3-7-55 - 1000